

The Influence of macro-roughness elements on the propagation of a bore over an initially dry bottom

Stefan Leschka, Hocine Oumeraci

Content

- Introduction
- Inundation modelling for tsunami early warning system in Indonesia
- Alternative approach
- Validation
- Setup
- Results
- Smmry, cnclsn, tlk



01.

Introduction

Introduction

- motivation: tsunami inundation modelling
- depth-averaged models (non-linear shallow water (NLSW) and Boussinesq models):
 - use Manning formula with coefficient for bottom
- Macro-roughness elements (buildings and tree vegetation):
 - too small to be represented in numerical grid/mesh
 - may be considered by increased Manning's coefficient

$$u = \frac{1}{n} R_b^{2/3} \sqrt{S_0}$$



not physically sound



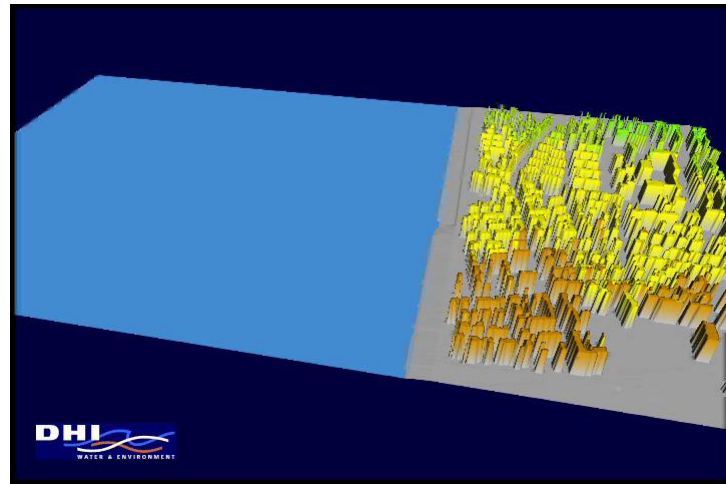
large uncertainties

02.

Inundation modelling for the Tsunami Early Warning System in Indonesia

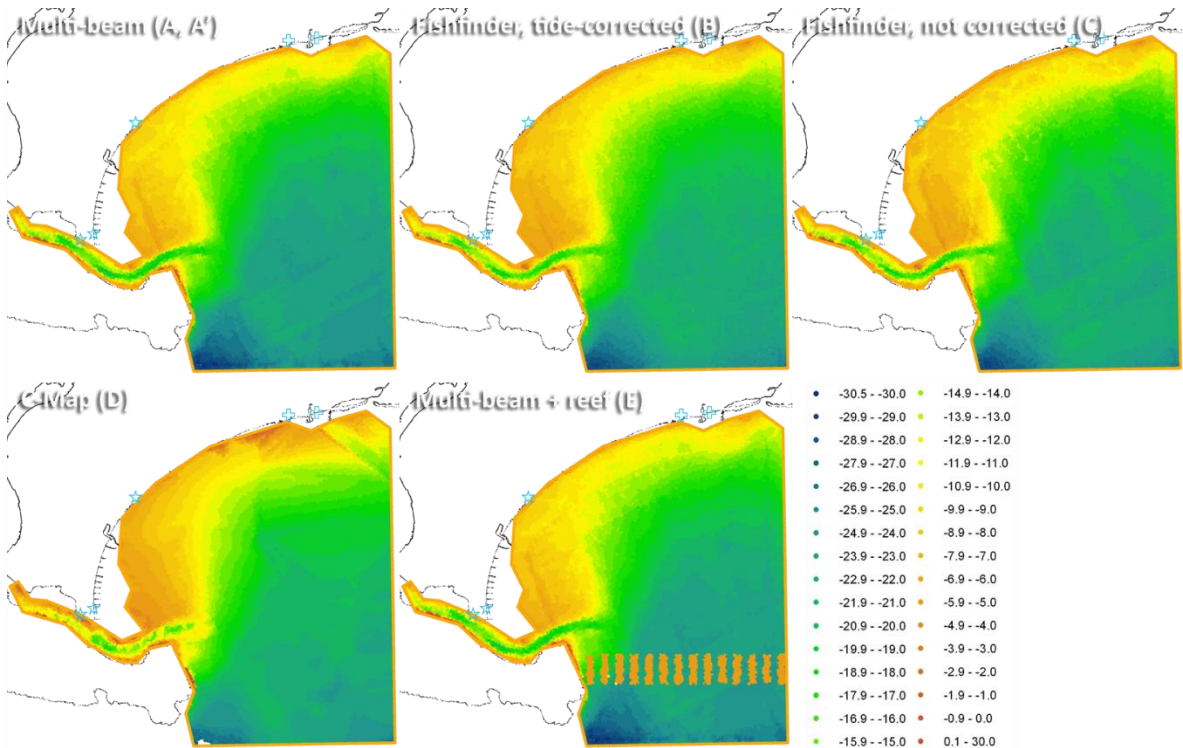
Modeling software

- 2D numerical models (non-linear shallow-water equation model, such as MIKE 21)
- Depth-dependent drag coefficient in quadratic friction law from Gauckler/Manning/Strickler formula
- high resolution required
- model distinguishes between area types (e.g. streets, houses, vegetation)
- Eddy viscosity



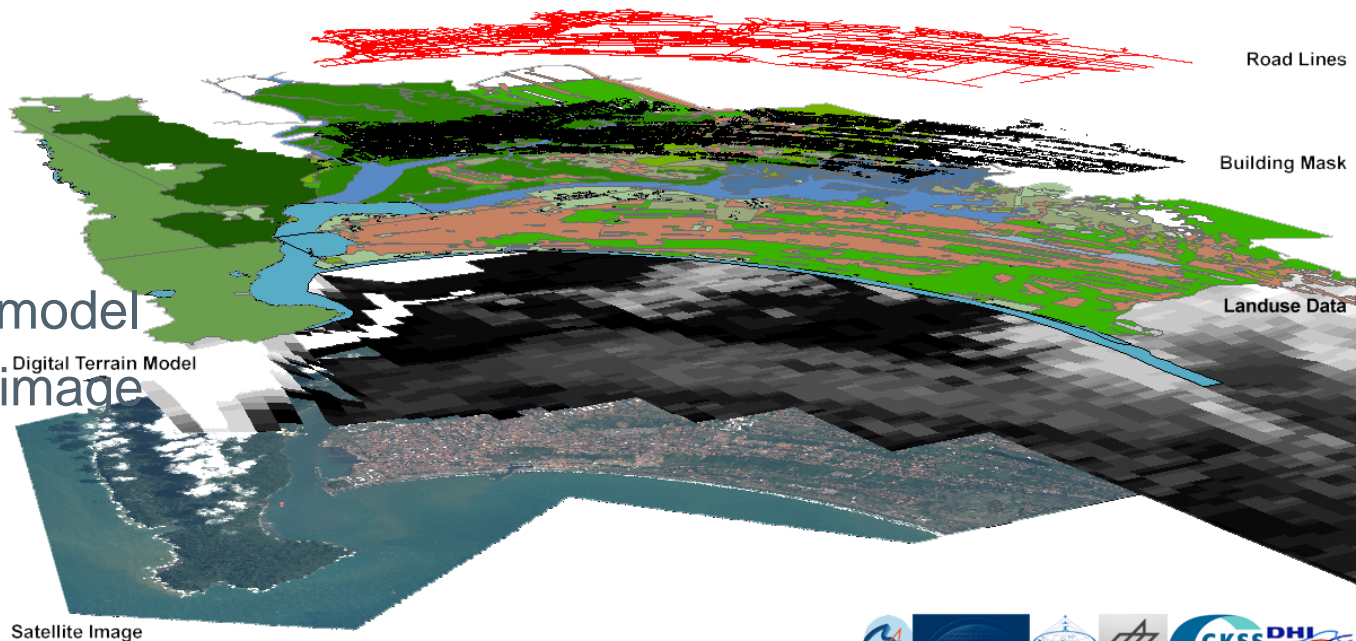
Bathymetry data

- Comparison of different data sets
- Runup does not vary significantly
(Leschka, Kongko & Larsen, 2009)



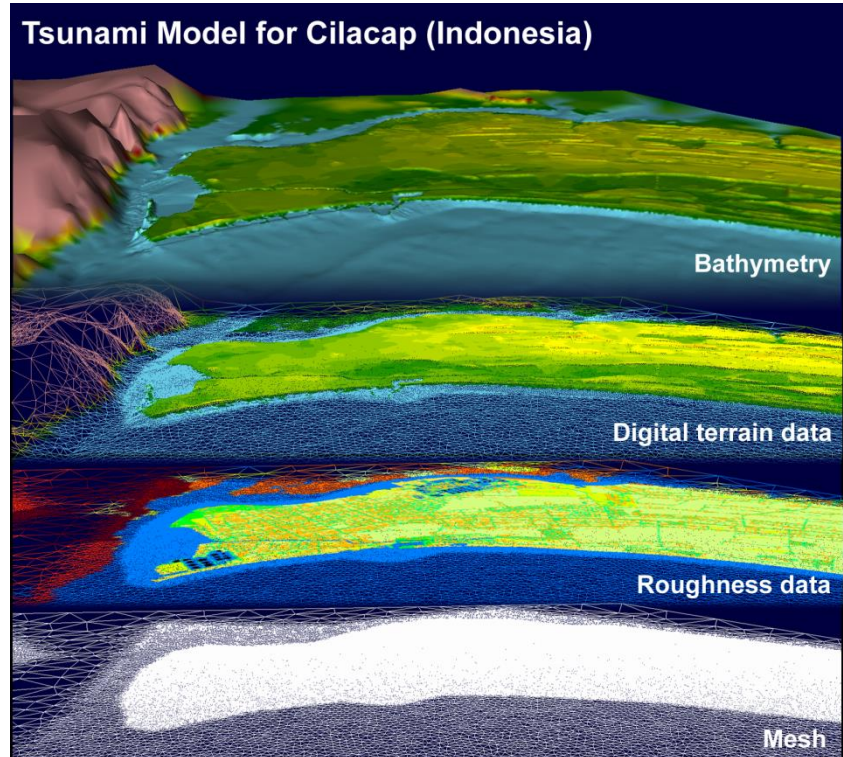
Roughness data

- Onshore:
 - Road lines
 - Building mask
 - Landuse data
 - Digital terrain model
 - Satellite/airial image



MIKE 21 FM setup

- Discretization: 2nd order time/space
- Timesteps: 0.01 – 10s ($CFL_{crit} = 0.8$)
- Drying/wetting/flooding:
0.005/0.05/0.1 m
- Eddy viscosity: Smagorinsky
- Bed resistance offshore: $32 \text{ m}^{1/3}/\text{s}$



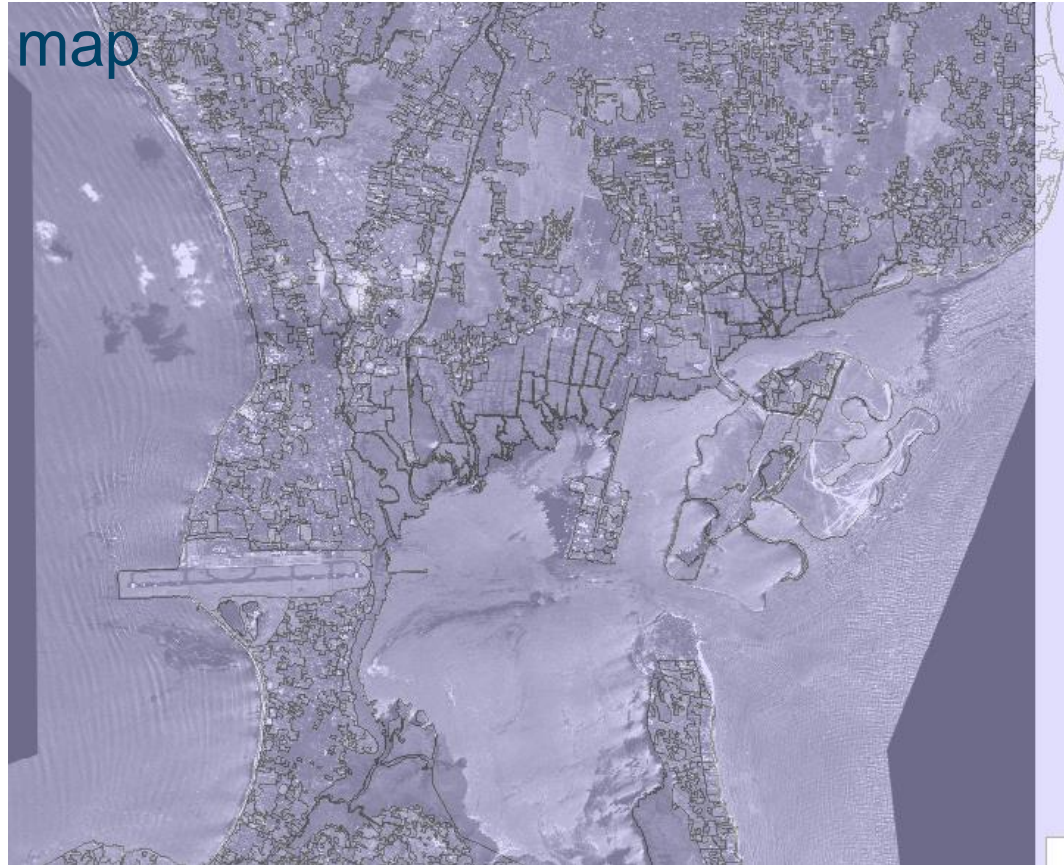
Generation of roughness map

- Digital Globe image (2006):
Quickbird Bali South



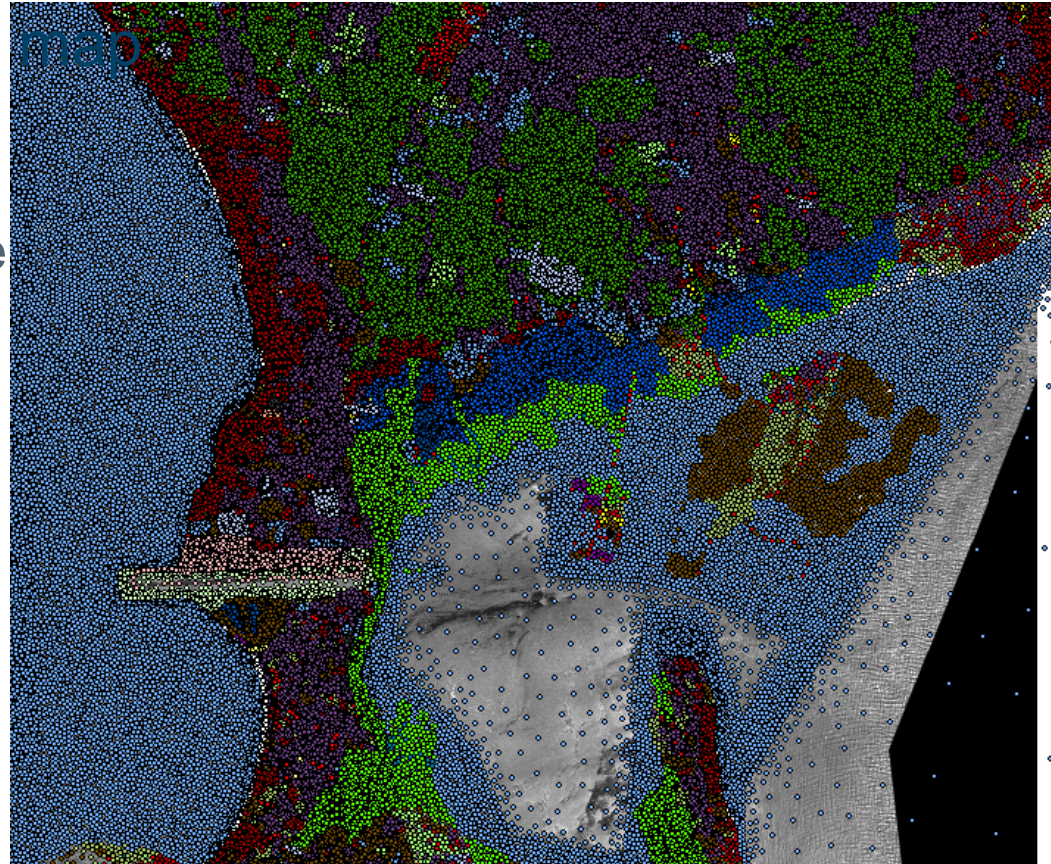
Generation of roughness map

- DLR (2008): Landuse Data
 - Hotel
 - Office area
 - Plantation
 - Industry
 - Settlement
 - Paddy field
 - Savannah



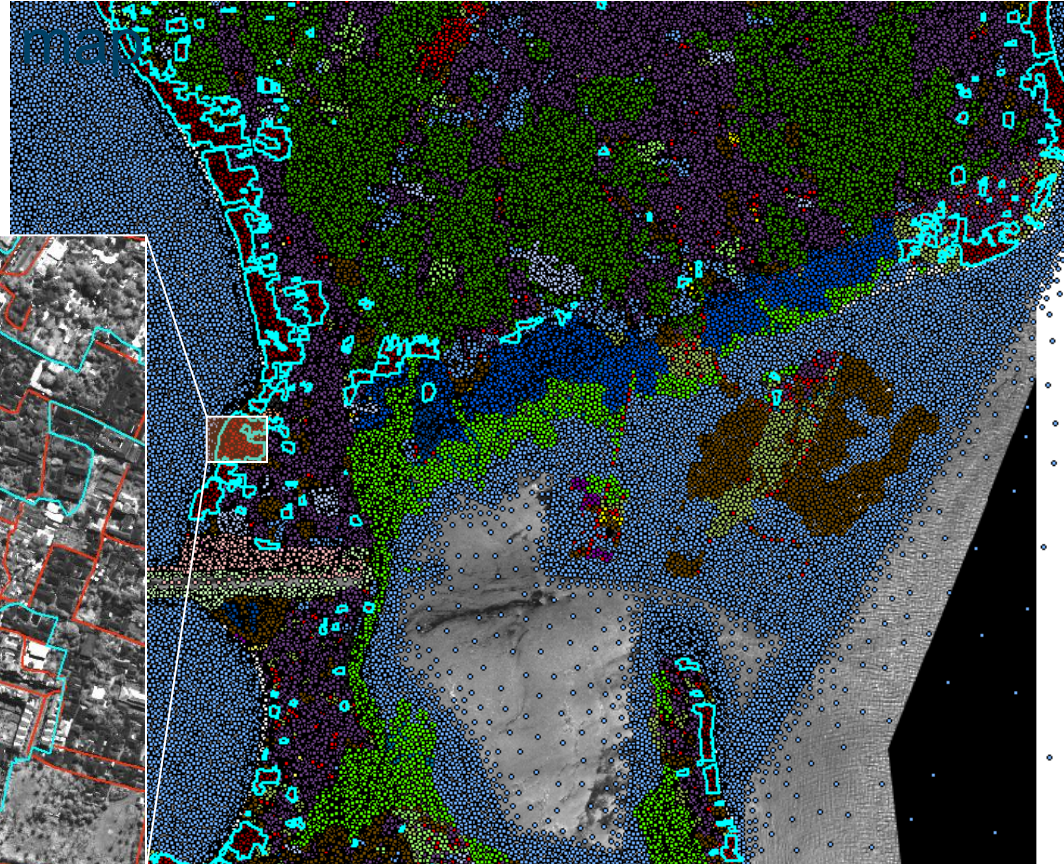
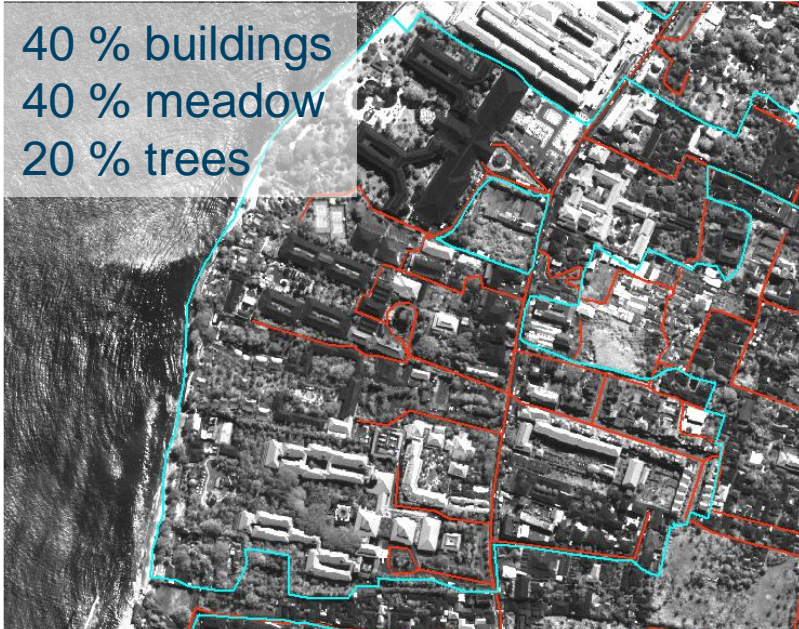
Generation of roughness map

- Splitted into fractions -> Manning no. From literature
 - sand
 - stone
 - soil
 - asphalt
 - meadow
 - Forest types



Generation of roughness map

- e.g. hotel areas:



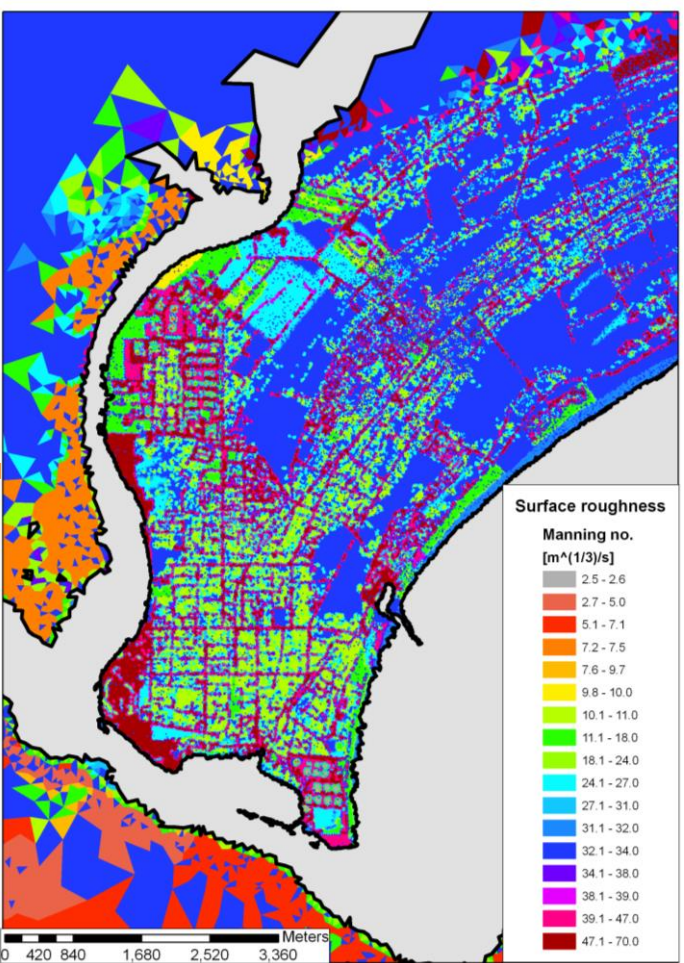
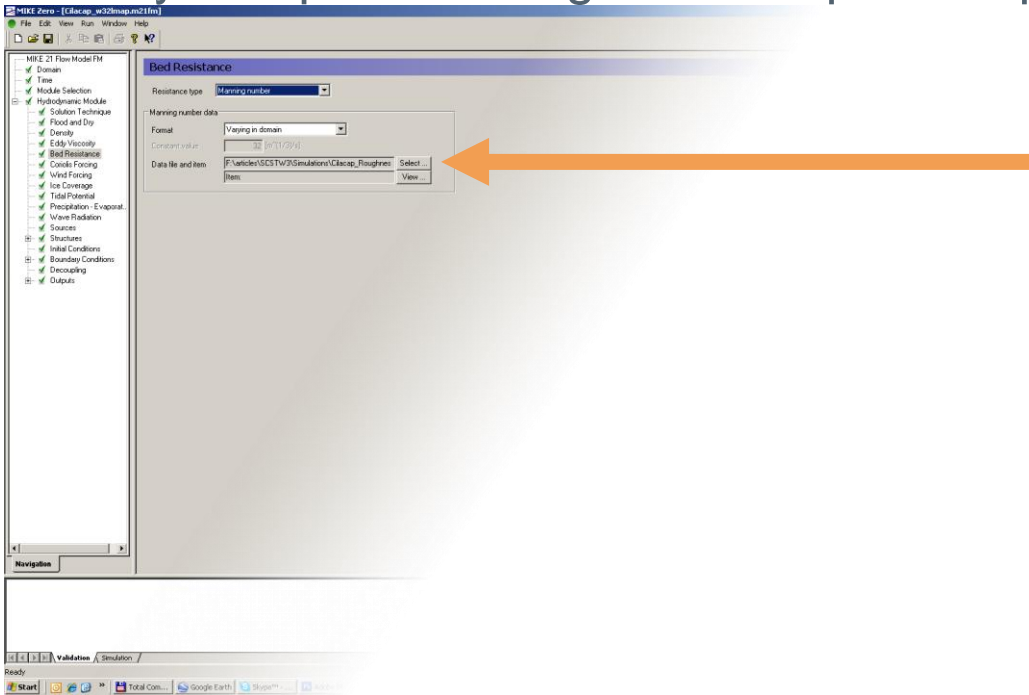
Generation of roughness map

- Buildings
 - resistant: $M = 2.5 \text{ m}^{1/3}/\text{s}$
 - non-resistant: $M = 11 \text{ m}^{1/3}/\text{s}$
- (Gayer, Leschka, Noehren, Larsen & Guenther, 2009. High resolution tsunami inundation modelling.
Annual meeting of AOGS, 11-15 August 2009, Singapore.



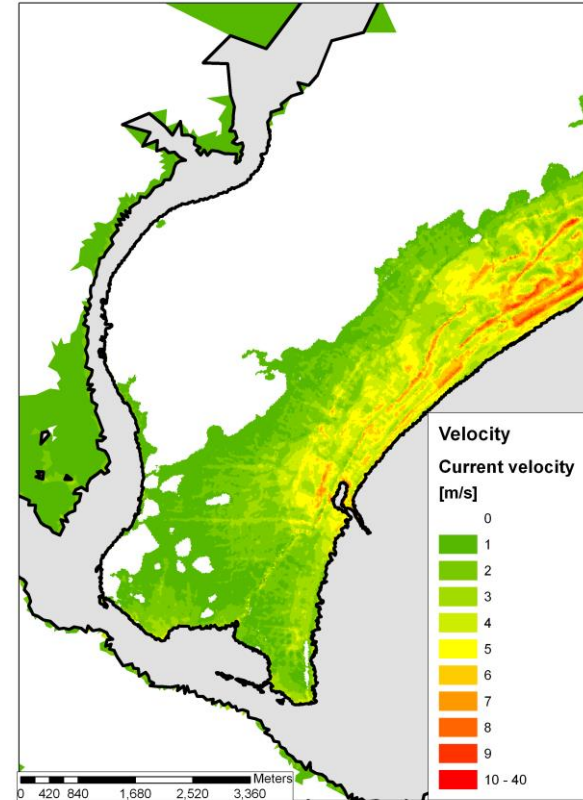
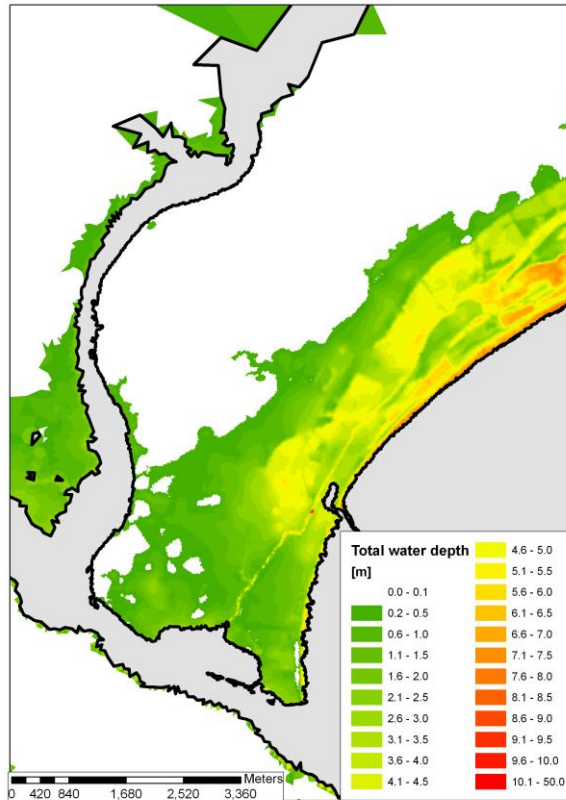
Generation of roughness map

- Linearly interpolated roughness map Cilacap



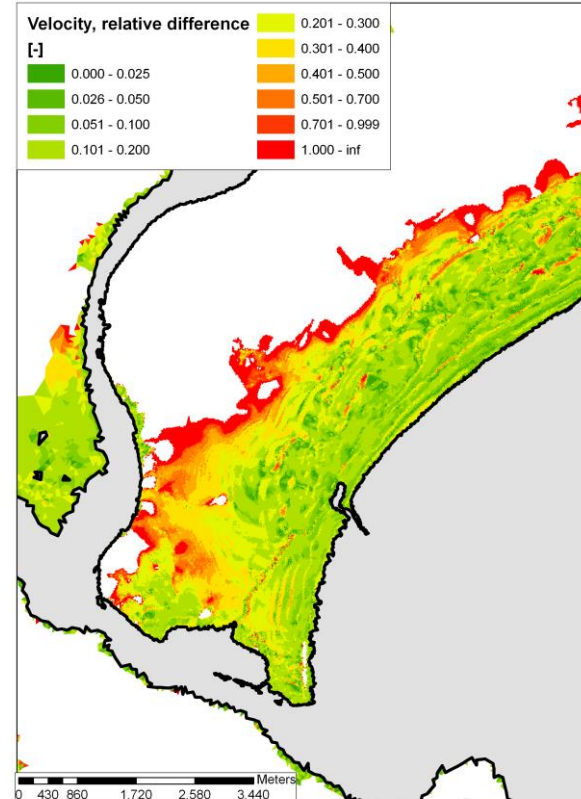
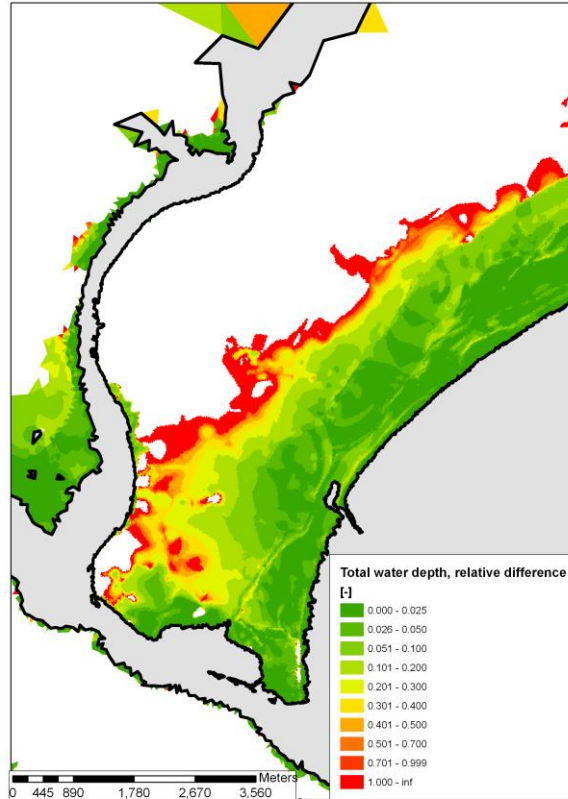
Example results

- total water depth
- current velocity

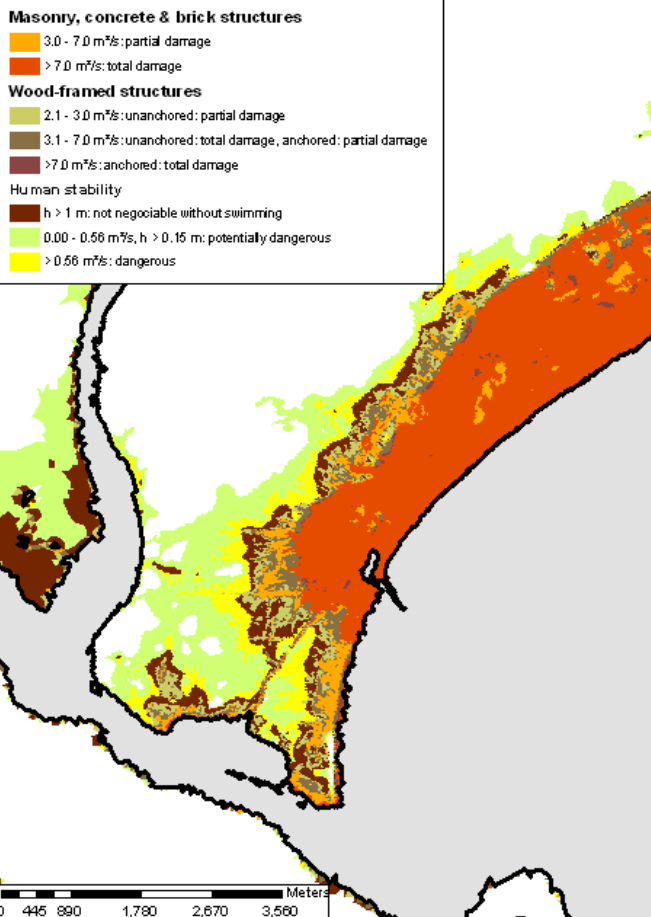
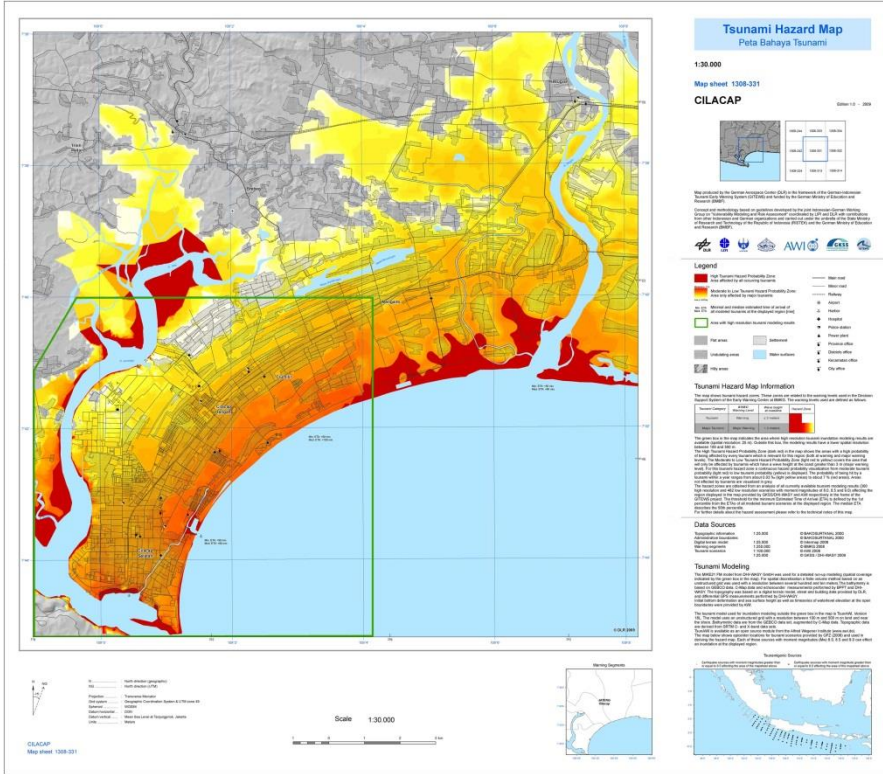


Sensitivity

- $M = 35 \text{ m}^{1/3}/\text{s}$
vs.
 $M = 5 \text{ m}^{1/3}/\text{s}$
- total water depth
- current velocity



Hazard



03.

Alternative approach

Energy losses

- Energy losses during tsunami inundation
 - Friction
 - Drag
 - Vortex
 - Inertia
- Friction: Chézy (1775), Gauckler/Manning/Strickler
 - no viscosity -> fully rough/fully turbulent conditions
 - R_b hydraulic radius (channel flow)
 - steady state
 - dimensional

$$u = \frac{1}{n} R_b^{2/3} \sqrt{S_0}$$

$$C_F = \frac{gn^2}{h^{1/3}}$$

Energy losses

- previous work:
 - river engineering
 - Li & Shen (1973)
 - Fisher & Reeve (1994)
 - proposed inertia coefficients
 - Noji et al. (1993)
 - Tsutsumi et al. (2000)
 - Harada & Kawata (2004)
 - extensions to NLSW model
 - Matsutomi et al. (2006)
- vegetated/urban areas:
 - Augustin et al. (2009)
 - Yuan & Huang (2009)
 - Suzuki & Arikawa (2010)
 - Husrin et al. (2011)
 - Huang et al. (2011)
 - Goseberg (2011)
 - Huthoff (2012)
 - Li et al. (2012)

Energy losses due to friction

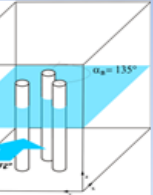
- Bradford & Sanders (2002): Manning approach near wet/dry boundary causes unrealistically large predictions of shear stress
- Haaland formula from pipe flow considers Reynolds number

$$C_F = \frac{0.204}{\ln^2 \left[\text{Re} + (k_s / 14.8h)^{1.11} \right]}$$

- still not applicable for vertical structures

Methodology

Phase 1: Model validation and plausibility tests



ANS-VOF model:
FOAM, laboratory scale

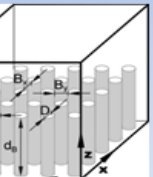
Flow condition:
solitary wave
bore



Near field: Far field:
- Forces - Flow velocities
- Water levels

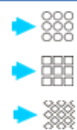
Basic understanding of influences of
- Arrangement
- distances
- Flow condition

Phase 2: Parameter study



ANS-VOF model:
FOAM, laboratory scale

Flow condition:
bore



Near field: Far field:
- Forces - Flow velocities
- Water levels
- Transmission coefficient
- Reflection coefficient
- Dissipation coefficient

understanding of influences of
- shape
- arrangement
- density
- submergence depth

Phase 3: Development of simple formulae

3D relations → empirical 2D relations

02.

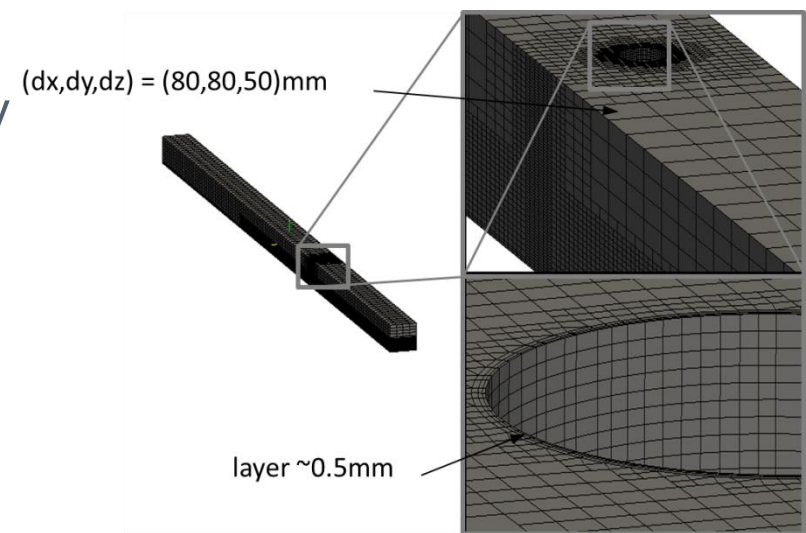
Model validation

Validation

- i. offshore:
 - a) forces on single cylinder due to regular waves (data by Bonakdar, 2012)
wave generation, propagation, force calculation
 - b) solitary wave heights (data by Strusinska, 2010)
numerical dissipation
- ii. onshore:
forces on single cylinder due to bore (Árnason, 2004)

Validation

- iii. interaction in a group of cylinders subject to regular waves
 - a) comparison with laboratory data (Bonakdar & Oumeraci, 2014)
 - b) plausibility tests with lab data (Bonakdar, 2012) and empirical relations



Mesh scene of the bore validation

Validation: i.b) Bore at a single cylinder

- tank of the Charles W. Harris Hydraulics Laboratory of the University of Washington
 - dimensions:
 $L / W / H = 16.62 / 0.61 / 0.45 \text{ m}$
 - column diameter $D_B = 0.14 \text{ m}$
 - impoundment height $h_0 = 0.25 \text{ m}$

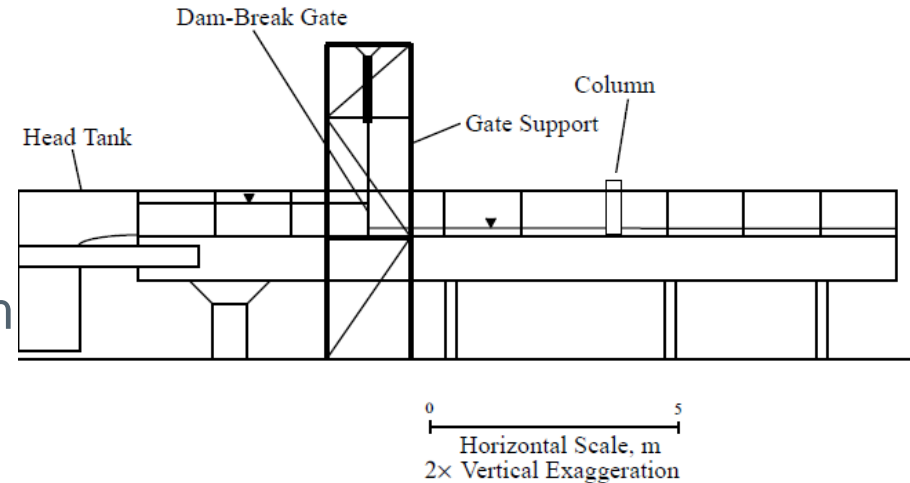
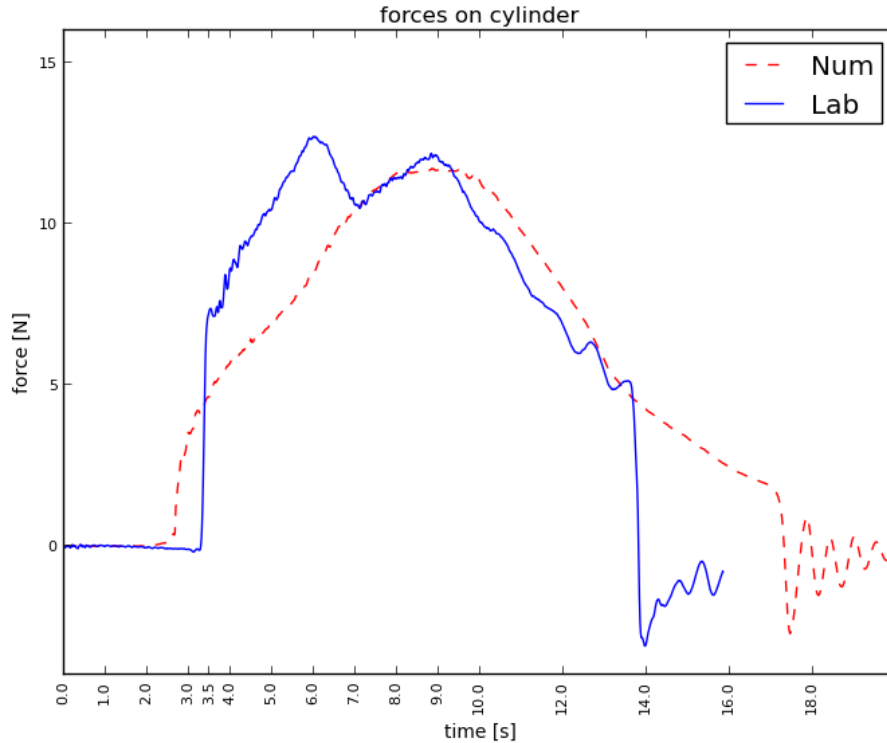


Figure 4.1: A diagram of the tank (adapted from Moore (1999))

source: Árnason (2004)

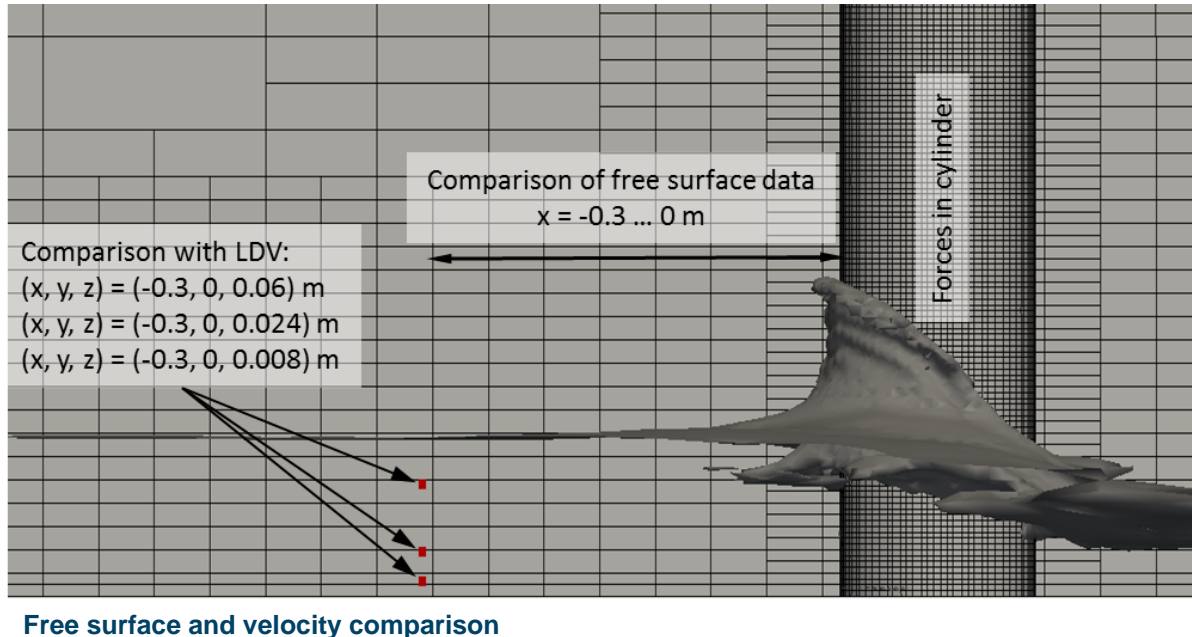
Validation: i.b) Bore at a single cylinder

- first result:



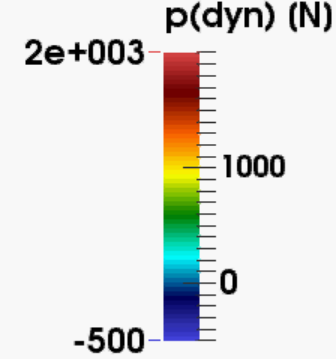
Validation: i.b) Bore at a single cylinder

- bore at a single cylinder (Árnason, 2004)



dry bottom

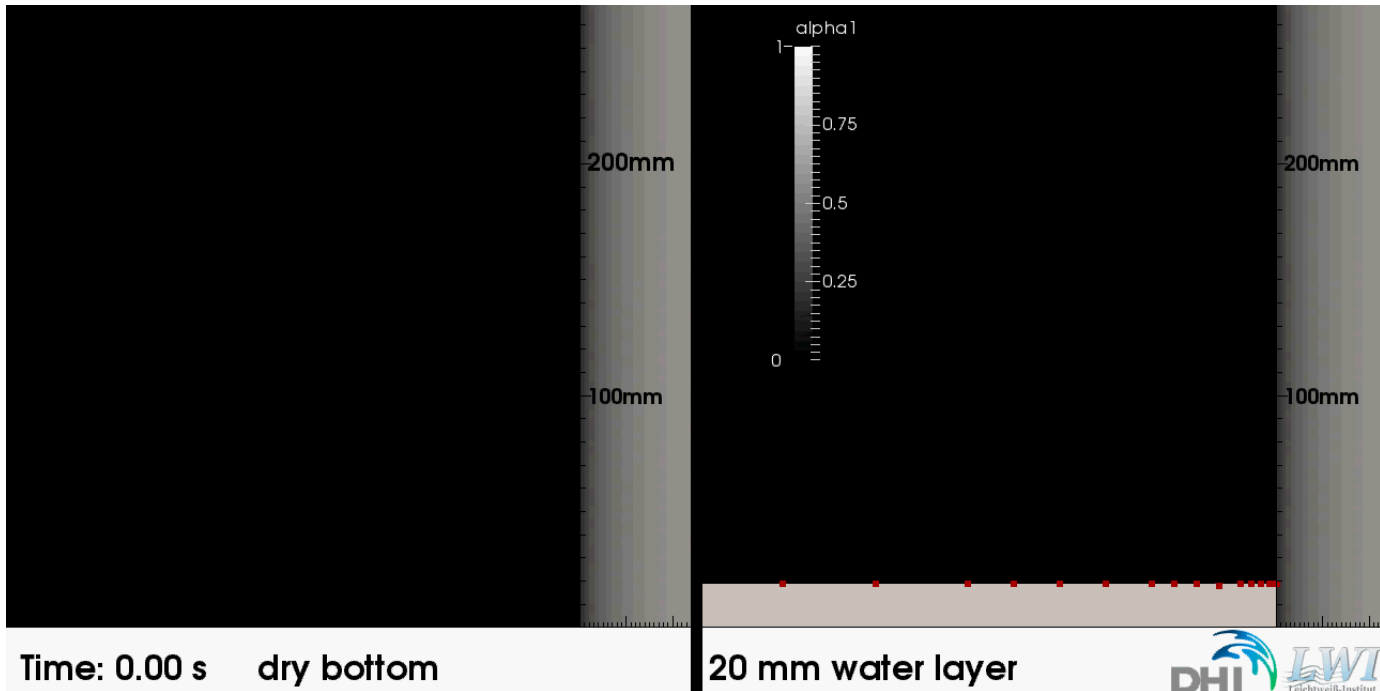
20 mm water layer



Validation: 1.b) Bore at a cylinder

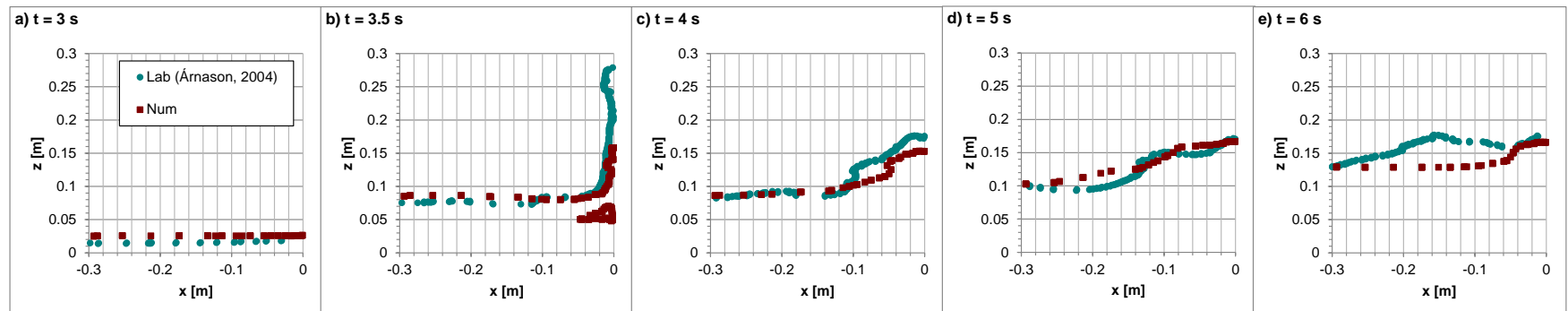
- Free surface in at upstream cylinder face

red dots: interpolated free surface
alpha1: simulated water phase content in cells



Validation: Bore at a single cylinder

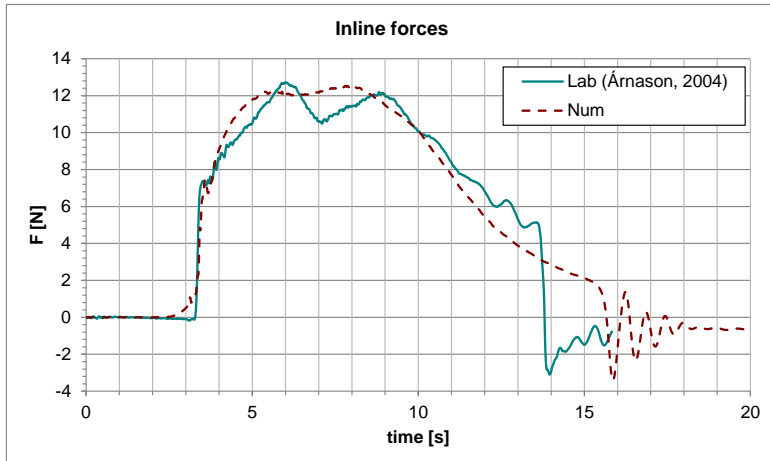
- Free surface data comparison



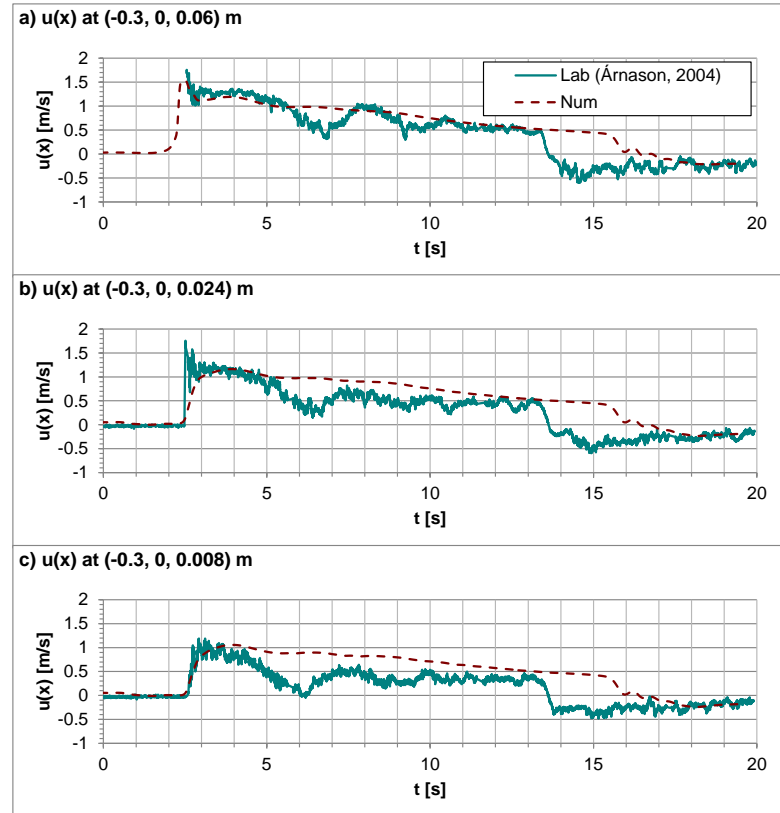
Free surface comparisons at different time steps.

Validation: Bore at a single cylinder

- Bore at a single cylinder
 - Deviation max. $F \sim 1.6\%$



Force comparisons at different time steps.



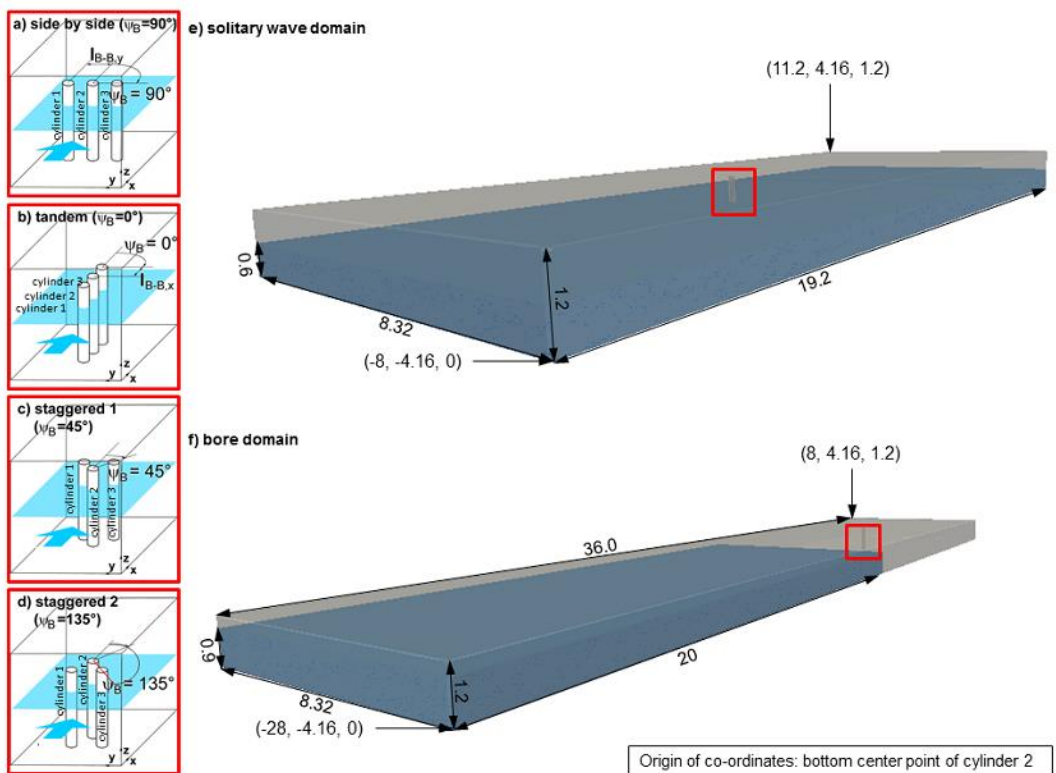
Velocity comparisons at different time steps.

03.

Setup

Setup

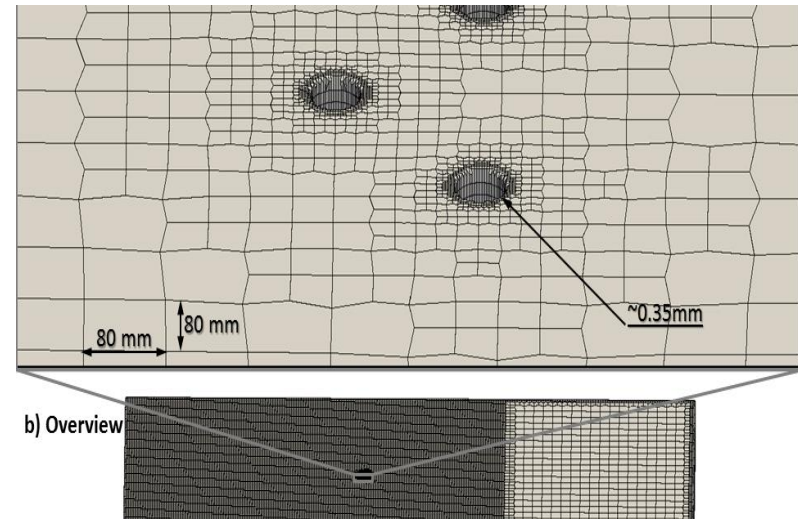
- Distances:
 - $0.5 D_B$
 - $1.0 D_B$
 - $2.0 D_B$
 - $3.0 D_B$
- arrangement angle Ψ_B :
 - spans clockwise between
 - main flow direction
 - direction of next roughness element



- **Basic arrangements of cylinders**

Setup

- 3D Navier-Stokes model:
OpenFOAM (OpenFOAM Foundation, 2010)
- wave cases:
 - wavesToFoam toolbox
(Jacobsen et al., 2012)
- bore cases:
 - interFoam solver



Mesh scene of wave cases

Setup

- numerical parameters:

Domain	Solitary wave	Bore
X	$\{-8, \dots, 11.2\}$ m	$\{-28, \dots, 8\}$ m
Y	$\{-4.16, \dots, 4.16\}$ m	$\{-4.16, \dots, 4.16\}$ m
Z	$\{0, \dots, 1.2\}$ m	$\{0, \dots, 1.2\}$ m
Mesh		
dx/dy	0.08 m (180 cells/L)	0.08 m
dz	0.01 m (22 cells/H)	0.01 m
initial/BC		
H	0.22 m	-
h_0	0.6 m	0.9 m

Methodology

- Normalize and analyze

- flow field

$$u(x)_{soliton,max}^* = \frac{u(x)_{soliton,max}}{u(x=0)_{soliton,no\ cylinder,max}}$$

- forces in cylinders

$$F(x)_{max}^* = \frac{F(x)_{i,max}}{F(x)_{single,max}}$$

04.

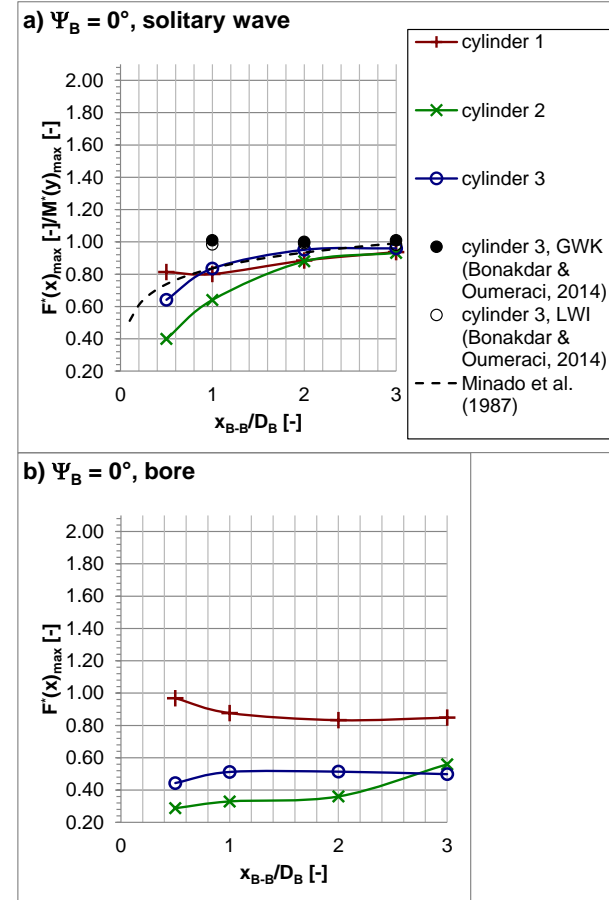
Results

Tandem

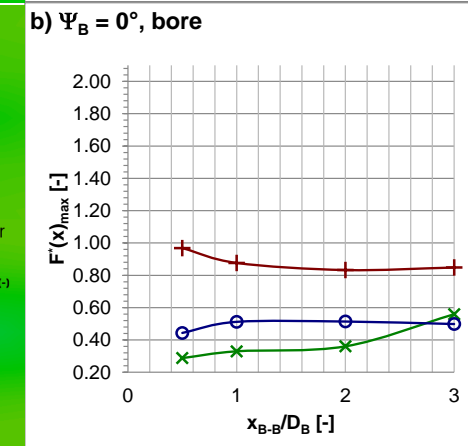
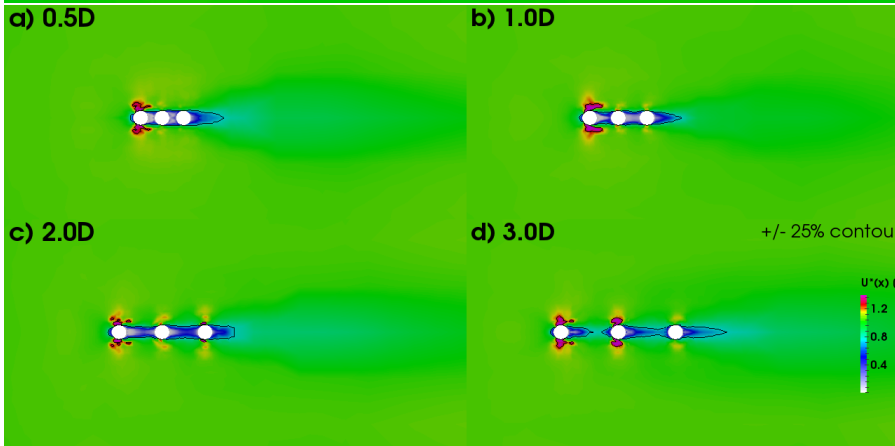
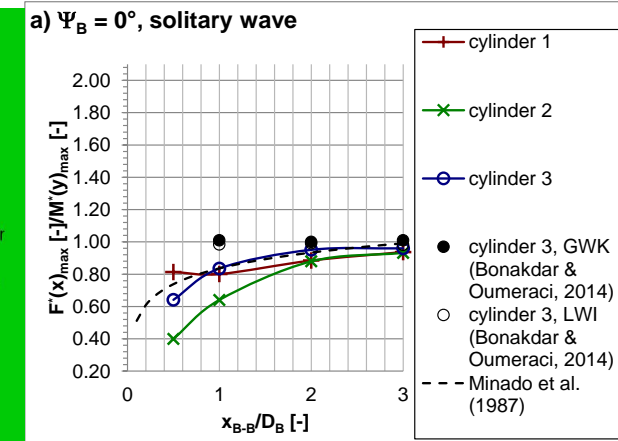
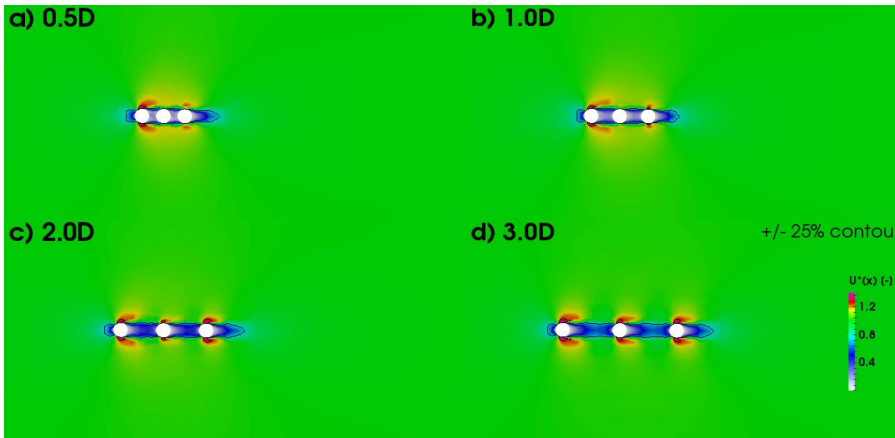


- tandem arrangement ($\Psi_B = 0^\circ$)
 - differences more pronounced in bore cases
 - distance
 - differences decrease with increasing distance
 - bores: plays minor role
 - solitary wave: at $3 D_B$, cylinders independent

Mindao et al. (1987): $K_z = 0.836 + 0.141 \ln(x_{B-B}/D_B)$



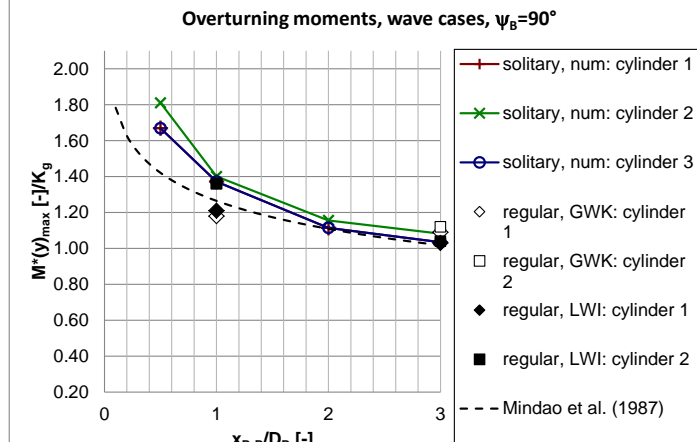
F^*_{\max} in three cylinders in tandem arrangement



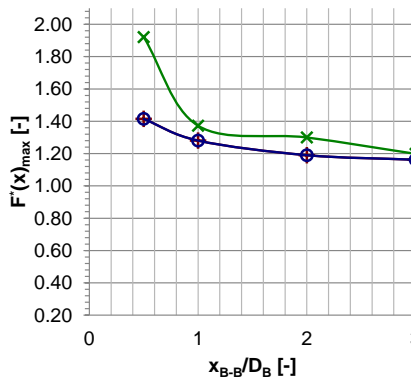
F^*_{max} in three cylinders in tandem arrangement

Side-by-side

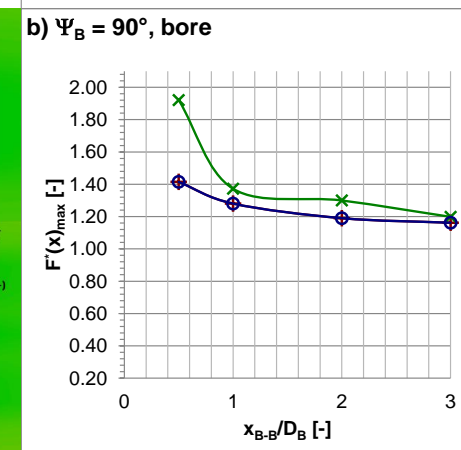
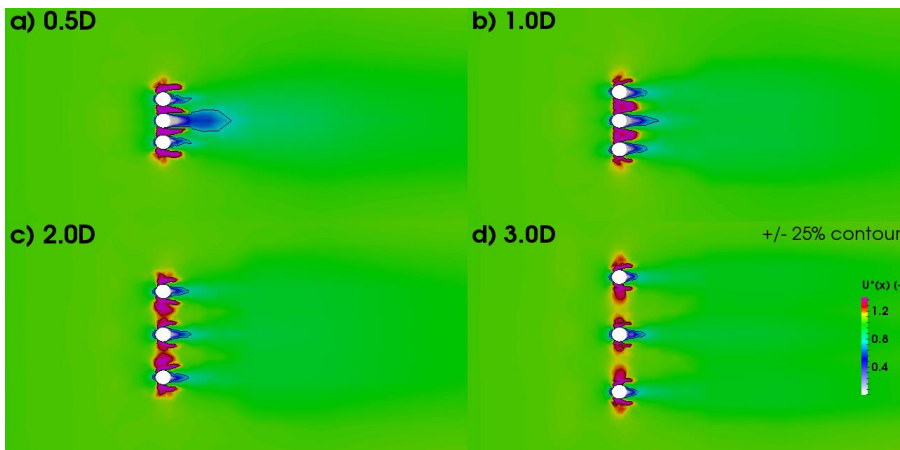
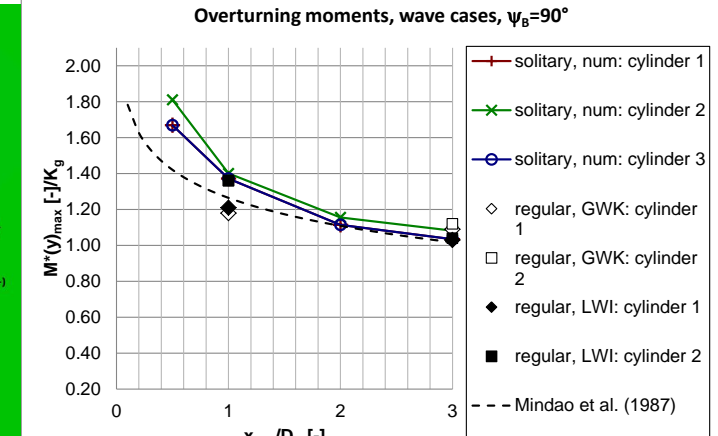
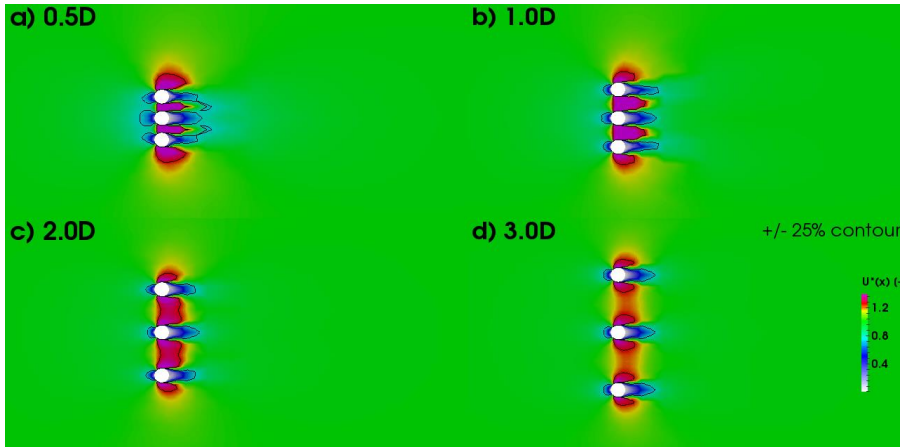
- side-by-side arrangement ($\Psi_B = 90^\circ$)
 - differences are more pronounced under bore conditions
 - distance:
 - solitary wave: at $3D_B$ cylinders act almost independent
 - bore: differences vanish, but at $3D_B$ cylinders receive higher load than single cylinder



b) $\Psi_B = 90^\circ$, bore



F_{\max}^* in three cylinders in side-by-side arrangement;
reg. wave case by Bonakdar & Oumeraci (2014)



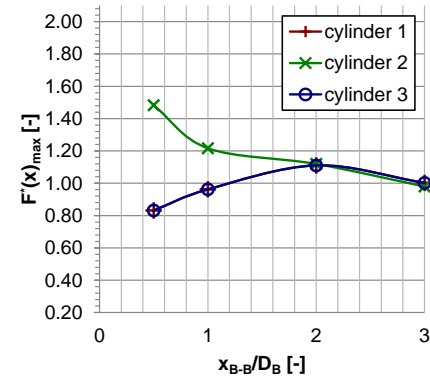
F_{\max}^* in three cylinders in side-by-side arrangement;
reg. wave case by Bonakdar & Oumeraci (2014)

Staggered 1

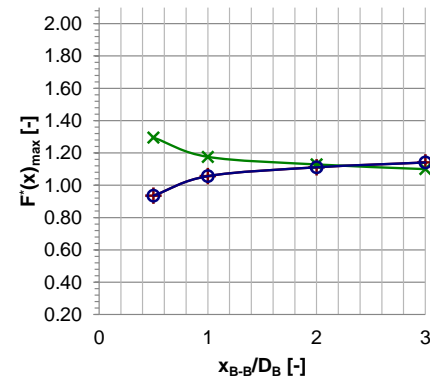


- staggered 1 arrangement ($\Psi_B = 45^\circ$)
 - differences are more pronounced under wave conditions
 - distance:
 - solitary wave: at $3D_B$, cylinders independent
 - bore: at $3D_B$ still interaction

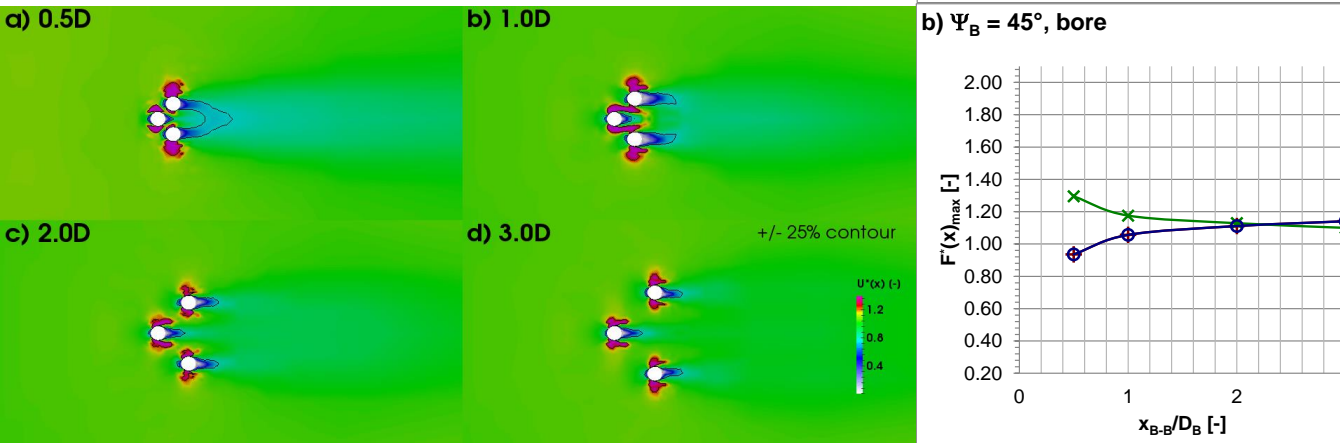
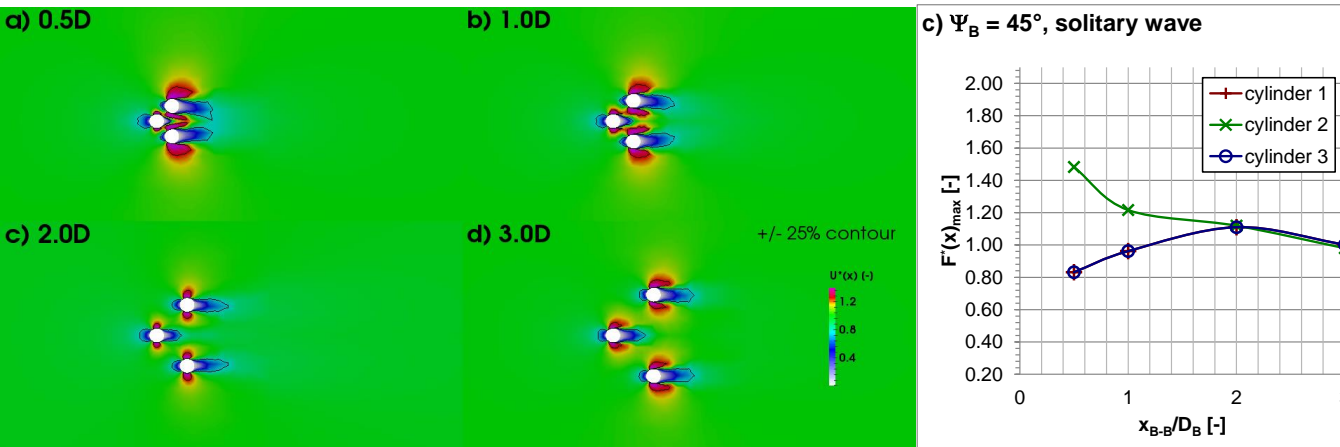
c) $\Psi_B = 45^\circ$, solitary wave



b) $\Psi_B = 45^\circ$, bore



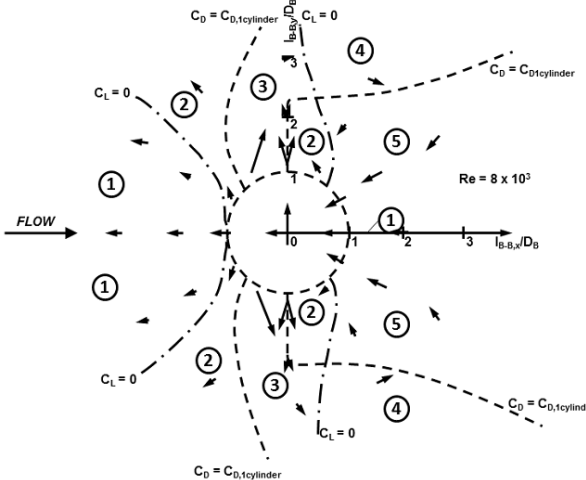
F^*_max in three cylinders in staggered 1 arrangement;
reg. wave case by Bonakdar & Oumeraci (2014)



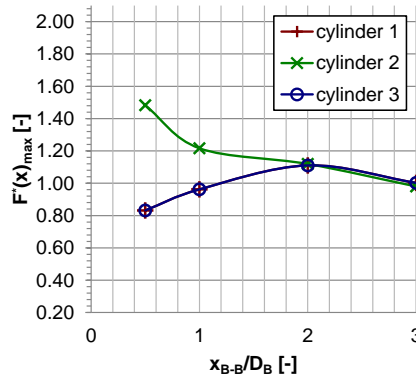
F^*_{\max} in three cylinders in staggered 1 arrangement;
reg. wave case by Bonakdar & Oumeraci (2014)



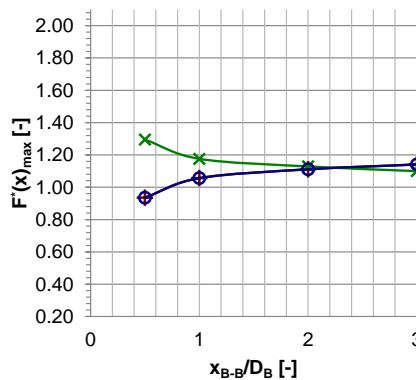
- staggered 1 arrangement ($\Psi_B = 45^\circ$)
 - modified from Hori (1959):



c) $\Psi_B = 45^\circ$, solitary wave



b) $\Psi_B = 45^\circ$, bore



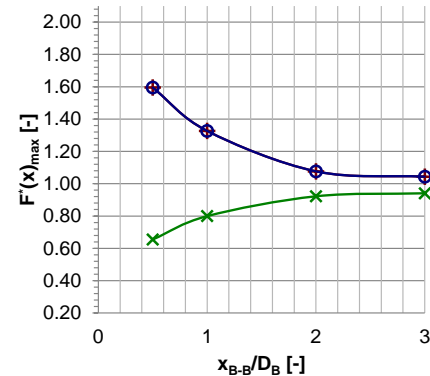
F'_max in three cylinders in staggered 1 arrangement;
reg. wave case by Bonakdar & Oumeraci (2014)

Staggered 2

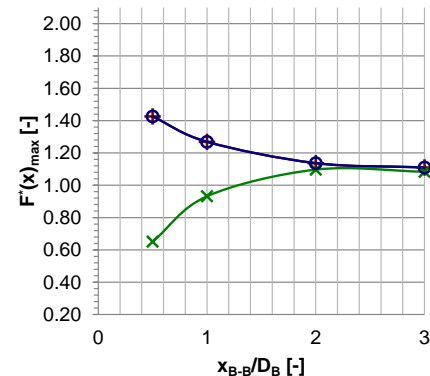


- staggered 2 arrangement ($\Psi_B = 135^\circ$)
 - differences are more pronounced under solitary wave conditions
 - distance:
 - solitary wave: at $3D_B$, small interaction
 - bore: at $2D_B$, small interaction, differences vanish

a) $\Psi_B = 135^\circ$, solitary wave

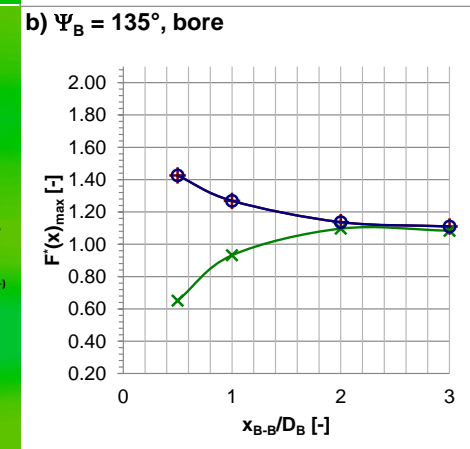
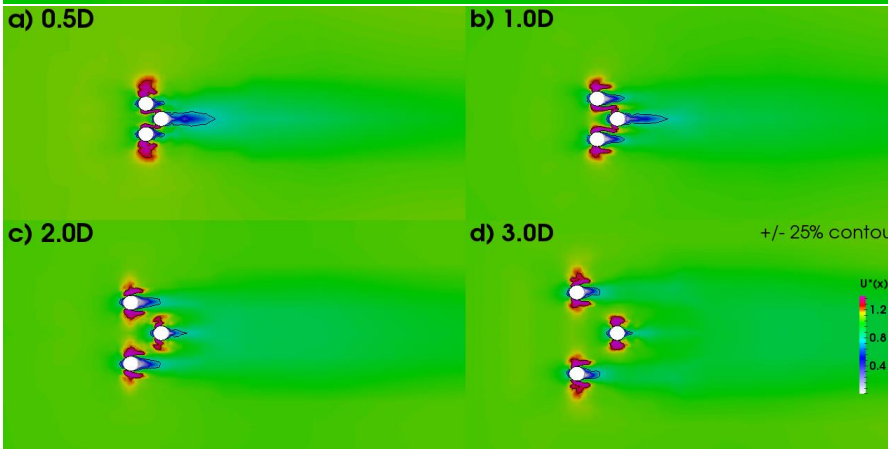
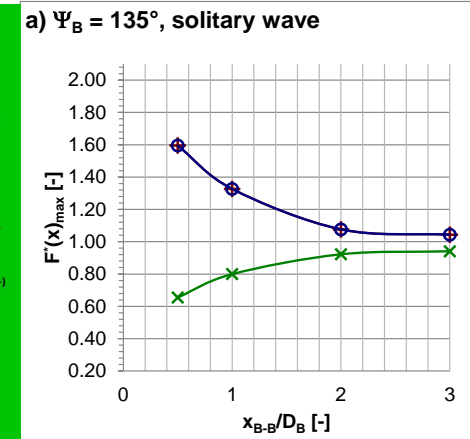
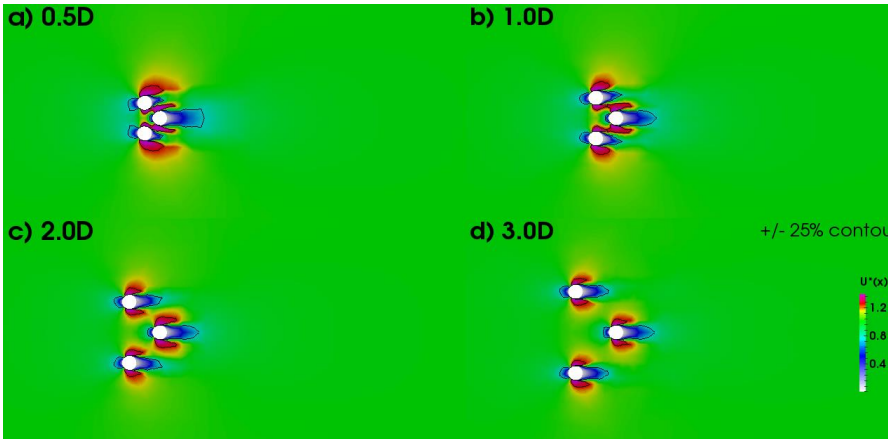


b) $\Psi_B = 135^\circ$, bore



Source: modified from Hori
(1959)

F^*_max in three cylinders in staggered 2 arrangement

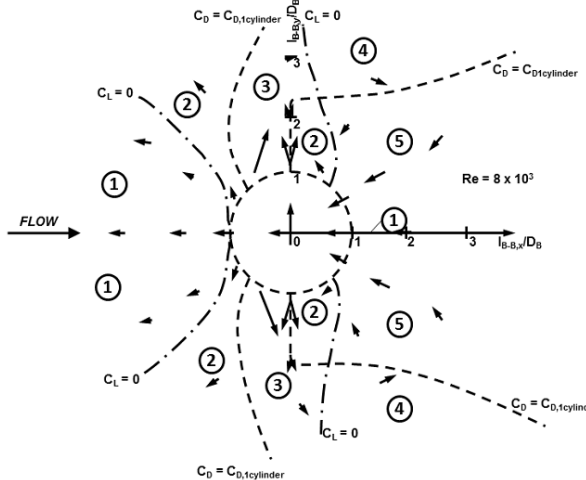


Source: modified from Hori (1959)

F^*_{max} in three cylinders in staggered 2 arrangement

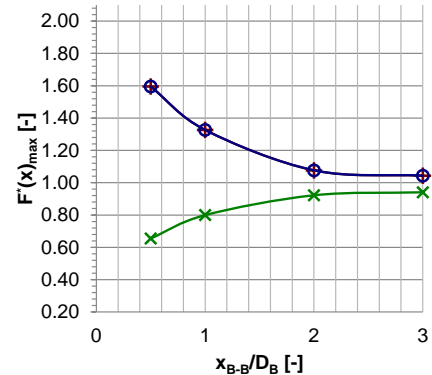


- staggered 2 arrangement ($\Psi_B = 135^\circ$)
 - modified from Hori (1959):

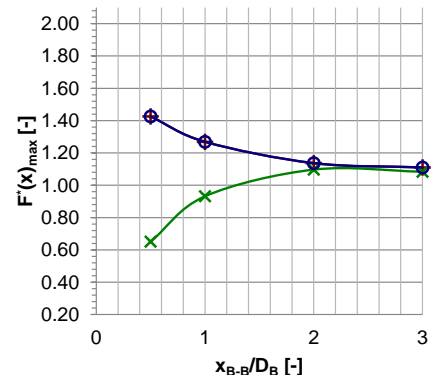


Source: modified from Hori
(1959)

a) $\Psi_B = 135^\circ$, solitary wave



b) $\Psi_B = 135^\circ$, bore



F^*_{\max} in three cylinders in staggered 2 arrangement

Results

- cylinder 1:

solitary wave						bore				
stdev	0	45	90	135	D _B	0	45	90	135	stdev
0.41	0.81	0.83	1.69	1.59	0.5	0.97	0.94	1.41	1.43	0.23
0.24	0.80	0.96	1.36	1.33	1	0.88	1.06	1.28	1.27	0.17
0.10	0.88	1.11	1.11	1.08	2	0.83	1.11	1.19	1.14	0.14
0.04	0.94	1.00	1.04	1.04	3	0.85	1.14	1.16	1.11	0.13
	0.06	0.10	0.25	0.22	stdev	0.05	0.08	0.10	0.13	

- cylinder 2:

solitary wave						bore				
stdev	0	45	90	135	D _B	0	45	90	135	stdev
0.58	0.4	1.48	1.81	0.65	0.5	0.29	1.29	1.92	0.65	0.62
0.31	0.64	1.22	1.4	0.8	1	0.33	1.18	1.37	0.93	0.39
0.12	0.88	1.12	1.15	0.92	2	0.36	1.13	1.3	1.1	0.36
0.06	0.93	0.98	1.08	0.94	3	0.56	1.1	1.2	1.08	0.25
	0.21	0.18	0.29	0.12	stdev	0.10	0.07	0.28	0.18	

- cylinder 3:

solitary wave						bore				
stdev	0	45	90	135	D _B	0	45	90	135	stdev
0.46	0.64	0.83	1.69	1.59	0.5	0.44	0.94	1.41	1.43	0.41
0.23	0.84	0.96	1.36	1.33	1	0.51	1.06	1.28	1.27	0.31
0.07	0.95	1.11	1.11	1.08	2	0.51	1.11	1.19	1.14	0.28
0.03	0.96	1	1.04	1.04	3	0.5	1.14	1.16	1.11	0.28
	0.13	0.10	0.25	0.22	stdev	0.03	0.08	0.10	0.13	

Results

- averaged standard deviations of solitary waves and bores for arrangement angle and distance

	solitary wave	bore
Ψ_B	0.22	0.30
x_{B-B}	0.18	0.11

- offshore conditions (solitary wave): both parameters have comparable influence
- onshore conditions (bore): arrangement dominates

05.

Summary, conclusion, outlook

Summary, conclusions

- 36 numerical experiments to quantify the importance of distance and arrangement between roughness elements
- model has been well validated (deviations to experimental data: < 2 %)
- numerical results agree well with laboratory data (Bonakdar & Oumeraci, 2014) and literature
- offshore conditions (solitary wave): distance and arrangement are of comparable importance
- onshore conditions (bore): arrangement dominates

Summary, conclusions

- loads on roughness elements result are related to energy losses in flow regimes offshore and onshore
- for empirical formulae in depth-averaged models
 - both parameters largely influence the results and need to be considered
 - especially for inundation modelling, the arrangement is of high importance

Outlook

- Almost finished systematic simulations of large groups of roughness elements investigating
 - size
 - height
 - arrangement
 - distance
- development of empirical formulae and implementation into NLSW model

Acknowledgements

- The authors like to thank
 - DHI Singapore for constant support
 - Lisham Bonakdar and Agnieszka Strusinska (TU Braunschweig) for data provision, open and fruitful discussions
 - Prof. Harry Yeh (Oregon State University) for data provision and very kind support
 - Dr. Ole Larsen (DHI) for very kind and constant support
 - Hisham El-Safti (TU Braunschweig) for open and fruitful discussions



Thank you for your kind attention!

DHI-WASY GmbH
Stefan Leschka
Max-Planck-Str. 6
28857 Syke
Germany

For further questions/feedback please e-mail to
sle@dhigroup.com

